



## Physical and optical parameter variation of modified borosilicate glasses

W. Awad<sup>a</sup>, A.M. Abdelghany<sup>b\*</sup>, M.S. Meikhail<sup>a</sup>

<sup>a</sup>Physics Department, Faculty of Science, Mansoura University, Mansoura, 35516, Egypt.

<sup>b</sup>Spectroscopy Department, Physics Research Institute, National Research Centre, 33 Elbehouth St., Dokki, 12311, Giza, Egypt

Received: 15/12/2021  
Accepted: 19/12/2021

**Abstract:** Modified borosilicate glasses of composition  $x\text{B}_2\text{O}_3 \cdot (45-x)\text{SiO}_2 \cdot 24.5\text{CaO} \cdot 24.5\text{Na}_2\text{O} \cdot 0.6\text{P}_2\text{O}_5$  were successfully synthesized using the melt quenching technique. Different physical parameters including density, molar volume, packing density, free volume, ion concentration, polaron radius, and average boron-boron distance were calculated and correlated to the optical energy gap calculated from UV/Vis. spectroscopic data. Dimitrov Sakka equation was also utilized to calculate the refractive index and dielectric permittivity.

**Keywords:** Borosilicate glass; Modified Hensch Bioglass; Density; UV/Vis. Spectroscopy

### 1. Introduction

Within the last decades, glasses utilized in multiple fields including engineering, medical agricultural technologies resulting from their unique characteristics. Recently, glasses used in electro - optic devices, thermos - mechanical sensors, biomedical applications, and reflecting windows. Glasses' qualities are inextricably linked to their composition and internal structural arrangement of their network [1–3]. Glass network generally comprises glass former, glass modifier, and flux. Mixed former borosilicate glasses are of researcher interest because of their lower heat of fusion compared to other silicate glasses. In addition, boron is characterized by their cations size, and high bond strengths with oxygen that allow borates to form exceptionally stable glasses with multiple stable configurations, including boron triangular and tetrahedral coordination's [ $\text{BO}_3$ , and  $\text{BO}_4$ ]. Boron is especially interesting to scientists because of its ability to the conversion of  $\text{sp}^2$  planar broxol structure [ $\text{BO}_3$ ] to stable  $\text{sp}^3$  tetra borate groups [ $\text{BO}_4$ ] [4]. One of the main characteristics of glasses is the wide range of optical absorption and other physical properties resulting from the composition and internal arrangement of their constituent oxides [5]. The absence of grain boundaries in the glassy network results from the intrinsic scattering loss of light that combined with glass transparency. A significant absorption result from electron

excitations appears when subjecting glasses to ultraviolet spectra [6]. Optical basicity is another method for analyzing the physicochemical properties of the glassy matrix. This method considers the electronic state of oxygen atoms in terms of electron donor power, which reflects the amount of negative charge carried. The nature and concentration of modifiers and intermediate oxides have a significant impact on the system entropy in glasses [7]. Even in normal conditions, however, borate glasses are durable and degraded with water vapor. Therefore, borosilicate glasses are employed to control and improve glass durability and degradation rates through the conversion of triangular borons to tetrahedral coordinated boron's  $\text{BO}_4$  [8]. The structure of silicate groups formed when  $\text{SiO}_2$  is incorporated into alkali borate glasses is found to be dependent on the concentration and distribution of a variety of units containing  $\text{BO}_3$  triangles and  $\text{BO}_4$  tetrahedral that are bonded to a variety of modifying oxide cations by non-bridging oxygen's (NBOs) or bridging oxygen's (BO) [9,10]. Extrinsic charge transfer and s-p absorption bands caused by metal ions that are impacted by the glass matrix, limit the true UV transmission of borosilicate glasses. Both intrinsic and extrinsic absorbance is crucial in revealing UV radiation-induced flaws in glasses [11]. Borosilicate glasses are used to make various coatings, semiconductor

microelectronics, optical lenses, enamels, solder glasses, glass-ceramic cement, and hard nuclear waste materials because they are chemically stable over a wide composition range, have low melting points, and a desirable electrical resistivity [12-16].

During the present work, the authors studied the effect of changing boron percentage within the modified Hench's 45S5 patent glasses. The work also extended to study several optical and structural parameters that correlated to the glass composition.

## 2. Experimental Work

### 2.1 Sample preparation

Glass samples were formed using analytical grade chemicals of Silicon dioxide SiO<sub>2</sub> supplied by LANXESS, Germany. Boron oxide used in the form of boric acid H<sub>3</sub>BO<sub>3</sub> supplied by El-Gomhouria Co. P<sub>2</sub>O<sub>5</sub> was introduced in the form of Ammonium dihydrogen orthophosphate supplied by LANXESS Co. CaO and Na<sub>2</sub>O were introduced in their carbonate form and supplied by EL-Nasr pharmaceutical chemicals Co. All previously mentioned chemicals were used to synthesize glassy samples with a composition shown in Table (1).

**Table (1)** Notation and structure of samples

Sample	Composition				
	SiO <sub>2</sub>	B <sub>2</sub> O <sub>3</sub>	CaO	Na <sub>2</sub> O	P <sub>2</sub> O <sub>5</sub>
B0	45	0	24.5	24.5	6
B5	40	5	24.5	24.5	6
B10	35	10	24.5	24.5	6
B15	30	15	24.5	24.5	6
B20	25	20	24.5	24.5	6
B25	20	25	24.5	24.5	6
B30	15	30	24.5	24.5	6
B35	10	35	24.5	24.5	6
B40	5	40	24.5	24.5	6
B45	0	45	24.5	24.5	6

The batches were melted in porcelain crucibles within a programmable electrical furnace regulated at 1100–1200 °C. Molten glass was occasionally stirred many times to ensure the formation of homogenized bubble-free glasses. To eliminate thermal and internal stresses, the molten glass was cast onto warmed stainless steel plates of the appropriate size, annealed for 1 hour, and then cooled gently to room temperature.

### 2.2. Physical measurements

Xylene was used as an immersion solvent to

determine the density of the examined glasses. The glass density ( $\rho$ ) was measured at room temperature (30 °C) using Archimedes' method. Using a digital balance, a bulk solid sample was weighed in air (WSA) and the solvent (WSL), and density was estimated as the average of triplicate readings using the formula [17]:

$$\rho = \frac{W_{SA}}{W_{SA} - W_{SL}} \rho_L \quad (1)$$

where  $\rho_L$  denotes sample density.

The predicted  $V_m$  of the synthesized glass samples:

$$V_m = \sum_i \frac{n_i M_i}{\rho} \quad (2)$$

where,  $M_i$  denotes the molecular mass of a component  $n_i$  denotes the molar ratio, and  $\rho$  is the sample density.

The  $V_f$  is used to describe molecular mobility within a network and is defined as the vacant space between molecules calculated using the formula:

$$V_f = V_m - \sum_i V_i X_i \quad (3)$$

The molar ratio of the samples is  $X_i$ , and the  $V_m$  of each component is  $V_i$ . The ratio of the ions' lowest fraction of volume occupied to the corresponding effective volume of glass computed using [18] was defined as Pd [19]:

$$Pd = \sum_i \frac{V_i X_i}{V_m} \quad (4)$$

The impact of dopant concentration in the glass matrix may also be evaluated using average boron–boron separation [20]:

$$d_{b-b} = \left[ \frac{V_m^b}{NA} \right]^{\frac{1}{3}} \quad (5)$$

where  $V_m^b$  is the boron atoms' molar volume and is provided by

$$V_m^b = \left( \frac{V_m}{2(1-X_b)} \right) \quad (6)$$

where  $X_b$  is the mole percentage of B<sub>2</sub>O<sub>3</sub> in the sample.

The ions concentration (N) is calculated using the formula [21]

$$N = \frac{\text{Mol\% of dopant} \times \text{Density of sample} \times \text{Avogadro's No}}{\text{Glass average molecular mass}} \quad (7)$$

A polaron is a quasi-particle that is used to characterize and grasp the interaction between ions and electrons in materials. Based on the

value obtained for N, the polaron radius ( $r_p$ ) in ( $\text{Å}$ ) may be calculated using the formula [22]:

$$r_p (\text{Å}) = \left(\frac{1}{N}\right)^{\frac{1}{3}} \quad (8)$$

These equations [23] can be used to calculate the field strength (F):

$$F = \frac{Z}{r_p^2} \quad (9)$$

where Z is the molar mass ( $\text{B}_2\text{O}_3$ ).

## 2.2 Optical constants

### 2.2.1 Optical energy gap ( $E_g$ )

Generally, two types of transitions can take place at the absorption edge of materials; a) direct and b) indirect transitions. According to Mott–Davis model [23], the formula is as the following:

$$(\alpha h\nu)^2 = B_1 (h\nu - E_{gd}) \quad (10)$$

$$(\alpha h\nu)^{1/2} = B_2 (h\nu - E_{gi}) \quad (11)$$

where  $h\nu$  is the photon energy,  $h$  is Planck's constant,  $E_{gd}$  is the direct bandgap,  $E_{gi}$  is the indirect band gap,  $B_1$ ,  $B_2$  are constants, and  $n$  is an integer. We can plot the relation between  $(\alpha h\nu)^2$  and  $(\alpha h\nu)^{1/2}$  as functions of energy ( $h\nu$ ) to obtain an optical bandgap.

### 2.2.2 Refractive index ( $n$ )

Refractive indices of the nanocomposites were calculated via the following formula [24, 25] and their values were listed in Table 1:

$$\frac{n^2-1}{n^2+2} = 1 - \sqrt{\frac{E_g}{20}} \quad (12)$$

### 2.2.3 Dielectric constant permittivity ( $\epsilon$ )

The dielectric constant permittivity of the sample glasses was calculated via the following formula:

$$\epsilon = n^2 - k^2 \quad (13)$$

$$k = \alpha\lambda/2 \quad (14)$$

where

$\alpha$ : linear absorption coefficient

$\lambda$ : wavelength of the absorption edge

## 3. Results and Discussion

### 3.1 UV-Visible Absorption Spectra of borosilicate glass

The optical absorption spectra of the glass samples within the spectral range extend from 200-1100 nm shown in Figure (1). The spectra characterized by two absorption bands within

the UV region at 250 and 320 nm previously correlated with the presence of iron impurities even in the ppm level and increasing boron content respectively. Calculations of the optical energy gap drawn from the fundamental absorption edge and both direct and indirect allowed transition drawn from the plotting of wavelength versus absorption, photon energy versus  $(\alpha h\nu)^2$ , and  $(\alpha h\nu)^{1/2}$  respectively as shown in Tauc's plots Figures (2, a, b and c) and (3, a, b and c) as an example for the energy gap calculations. In addition, the obtained optical energy gaps and calculated refractive index and dielectric permittivity were listed in the table (2). The correlation of the optical energy gap with both refractive index and dielectric permittivity is shown in Figure (3. a, b).

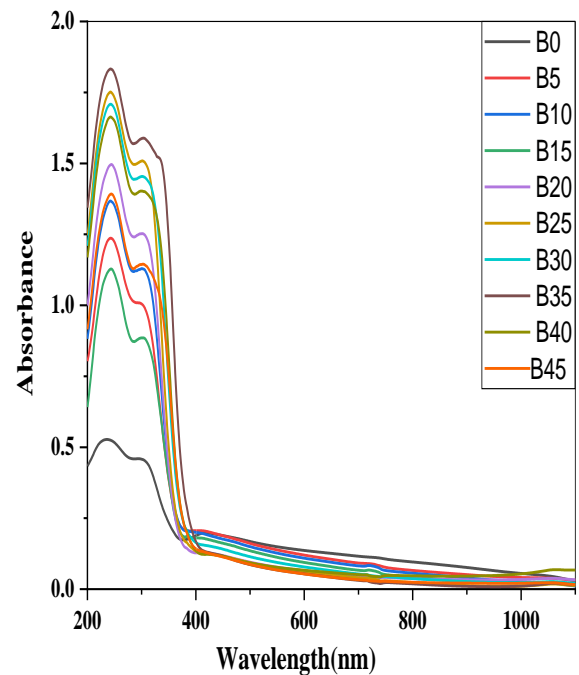


**Figure (1)** UV-vis experimental data for borosilicate glass

The density of the investigated samples decreases due to the increase of  $\text{B}_2\text{O}_3$  wt. % (from 0.0 to 45 wt. %). This increase can be explained based on the lower atomic weight of B (atomic weight,  $Z_B = 10.81 \text{ g mol}^{-1}$ ) as compared to Si (atomic weight,  $Z_{Si} = 28.09 \text{ g mol}^{-1}$ ). Moreover, the density of  $\text{B}_2\text{O}_3$  ( $2.46 \text{ g cm}^{-3}$ ) is higher than  $\text{SiO}_2$  ( $2.65 \text{ g cm}^{-3}$ ), leading to a decrease in the density of the prepared samples.

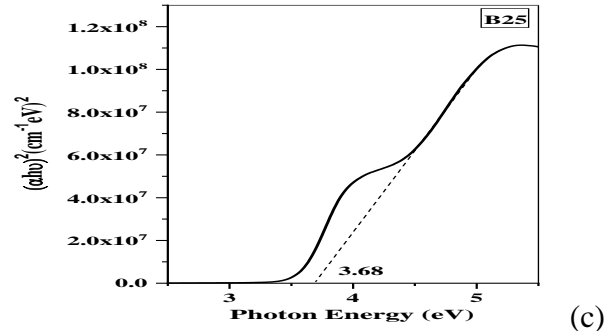
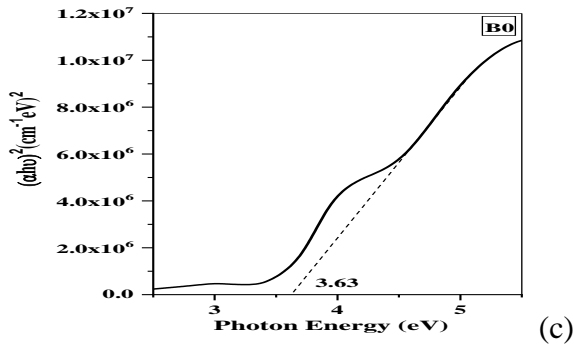
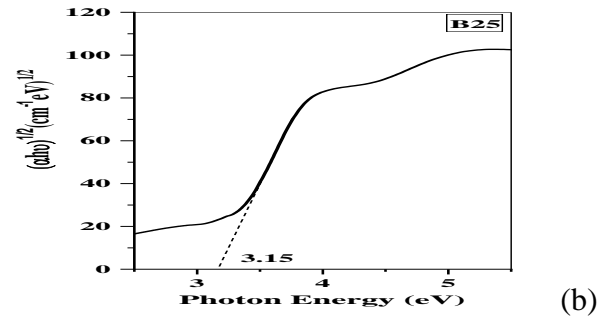
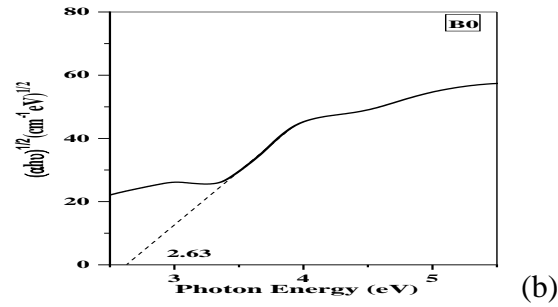
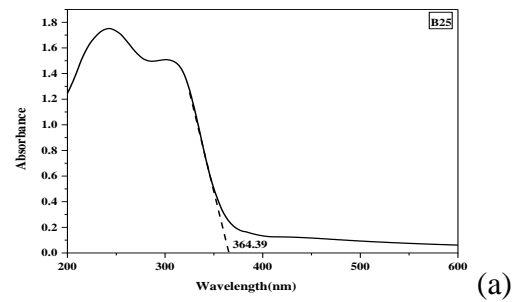
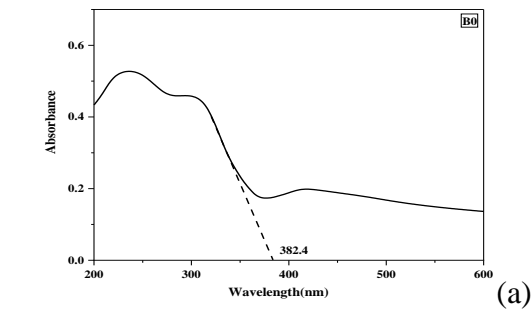


**Figure (2)** Tauc's plots used for energy gap calculations of sample B0

**Figure (3)** Tauc's plots used for energy gap calculations of sample B25

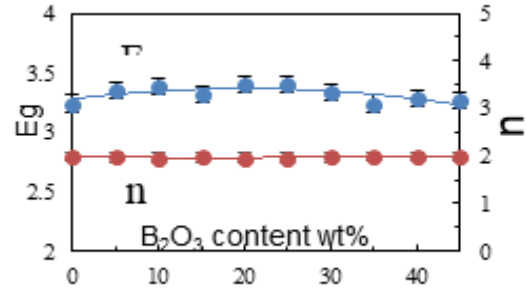
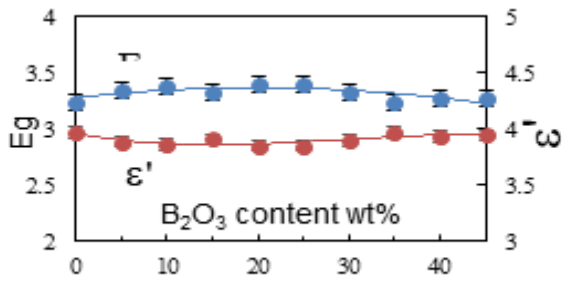


**Figure (4)** Optical energy gap, dielectric permittivity, and refractive index of studied glass

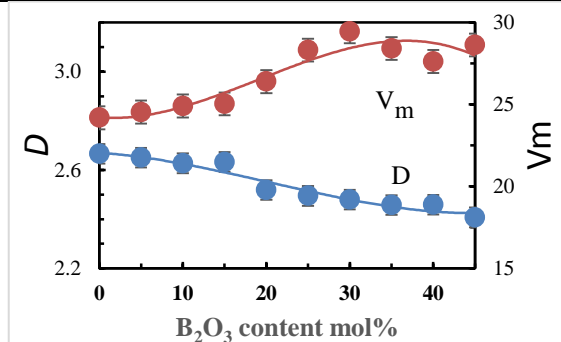
**Table 2** Calculated Energy gaps, refractive index, and dielectric permittivity

Sample	Boron Content	$\lambda_{\text{edge}}$ (nm)	$E_{\text{Optical}}$	$E_{\text{Direct}}$	$E_{\text{Indirect}}$	n	$\epsilon'$
			(eV)				
B0	0.0	382	3.24	2.63	3.63	1.99	3.97
B5	0.5	370	3.35	3.01	3.86	1.97	3.89
B10	10	367	3.38	3.05	3.88	1.97	3.87
B15	15	373	3.32	2.98	4.01	1.98	3.91
B20	20	364	3.40	3.11	3.89	1.96	3.85
B25	25	364	3.40	3.15	3.68	1.96	3.85
B30	30	372	3.33	3.08	3.74	1.98	3.9
B35	35	382	3.24	3.06	3.68	1.99	3.97
B40	40	377	3.28	3.06	3.8	1.98	3.94
B45	45	379	3.27	3.01	3.89	1.99	3.95

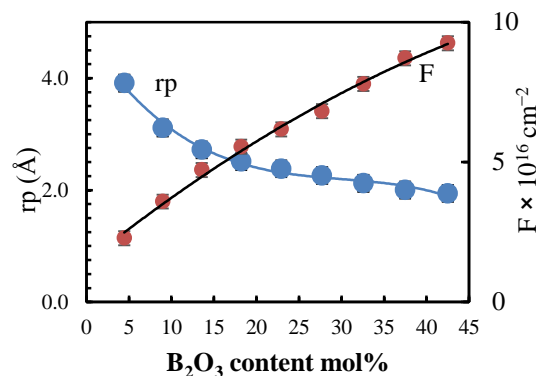
**Table (3)** reveals calculated physical parameters correlated to the structural variations in the synthesized glassy matrix after the change in the boron content at expense of the silicon partner.

**Table 3** Physical properties of  $x\text{SiO}_2-(45-x)\text{B}_2\text{O}_3-24.5\text{CaO}-24.5\text{Na}_2\text{O}-6\text{P}_2\text{O}_5$  glasses system

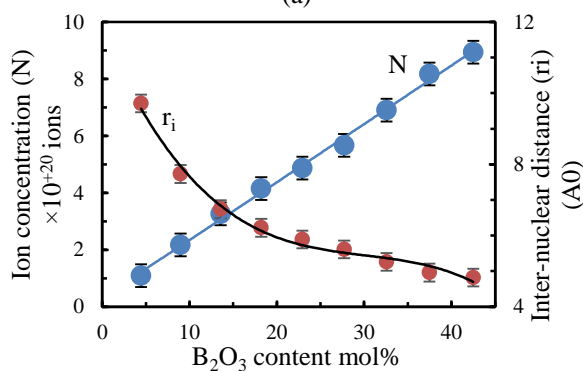
Parameters	Glass code									
	B0	B5	B10	B15	B20	B25	B30	B35	B40	B45
Density ( $d_s$ ) $\text{g cm}^{-3}$ $\pm 0.0002$	2.41	2.65	2.62	2.63	2.51	2.49	2.48	2.46	2.46	2.46
Molar volume ( $V_m$ ) $\text{cm}^3$ $\text{mol}^{-1} \pm 0.0001$	24.19	24.53	24.90	25.04	26.39	28.32	29.45	28.41	27.62	28.63
Packing density ( $P_d$ )	0.53	0.54	0.54	0.55	0.53	0.51	0.50	0.53	0.56	0.55
Free volume ( $V_f$ )	11.32	11.37	11.44	11.27	12.32	13.93	14.74	13.38	12.27	12.94
Average mol.wt. ( $M_{Av}$ ) (g)	58.23	65.01	65.43	65.91	66.47	70.65	73.02	69.83	67.92	76.33
Ion concentration ( $N$ ) ( $10^{+21}$ ions)	0.00	1.09	2.17	3.26	4.15	4.87	5.67	6.90	8.17	8.94
Polaron radius ( $r_p$ ) ( $\text{Å}^\circ$ )	0.00	3.91	3.11	2.72	2.51	2.38	2.26	2.12	2.00	1.94
Inter-nuclear distance ( $r_i$ ) ( $\text{Å}^\circ$ )	0.00	9.71	7.73	6.74	6.22	5.89	5.61	5.26	4.96	4.82
Field strength ( $F$ ) $10^{+17}(\text{g mol}^{-1}\text{cm}^{-2})$	0.00	2.28	3.59	4.72	5.55	6.17	6.82	7.79	8.71	9.25
Molar volume of the boron atoms $V_b$	12.09	12.84	13.68	14.48	16.14	18.37	20.37	21.07	22.09	24.89
Average boron-boron distance ( $d_{B-B}$ ) (nm)	1.26	1.27	1.272	1.274	1.29	1.33	1.35	1.33	1.32	1.33



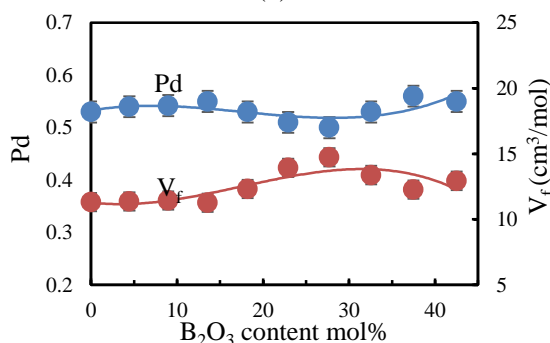
(a)



(b)



(c)



(d)

**Figure (5)** Calculated physical parameters versus boron content

#### 4. Conclusions

Modified borosilicate glasses of composition  $x\text{B}_2\text{O}_3-(45-x)\text{SiO}_2-24.5\text{CaO}-24.5\text{Na}_2\text{O}-6\text{P}_2\text{O}_5$  were successfully synthesized using the melt quenching technique. Several physical parameters including density, molar volume, packing density, free volume, ion concentration, polaron radius, and average

boron-boron distance were estimated and correlated to the experimentally found optical energy gap. It was noticed that variation in the boron content at expense of silicon dioxide is heavily affecting all physical parameters of the synthesized glasses. Synthesized glasses were recommended to be used as core fiber optical waveguide cladding material since they have a

low optical loss in the red and infrared portions of the spectrum.

## 5. References

- Subbalakshmi P., N. Veeraiah (2002), Study of  $\text{CaO-WO}_3\text{-P}_2\text{O}_5$  glass system by dielectric properties, IR spectra and differential thermal analysis. *Journal of non-crystalline solids*, **298(1)**, 89-98.
- K. S. Sharma, V. Rajendran, K. Singh, A.V. Gayathri Devi, S. Aravindan, (2006). Structural and acoustic investigations of calcium borate glasses. *physica status solidi (a)*, **203(10)**, 2356-2364.
- Sharma G., K.S. Thind, H. Singh, L. Gerward (2007), Optical properties of heavy metal oxide glasses before and after g- irradiation. *physica status solidi (a)*, **204(2)**, 591-601.
- Kaur G., O.P. Pandey, K. Singh (2012). Effect of modifiers field strength on optical, structural and mechanical properties of lanthanum borosilicate glasses. *Journal of Non-Crystalline Solids*, **358(18-19)**, 2589-2596.
- Gahlot P.S., V.P. Seth, A. Agarwal, N. Kishore, S.K. Gupta, M. Arora, D.R. Goyal (2004), Influence of ZnO on optical properties and dc conductivity of vanadyl-doped alkali bismuthate glasses. *Radiation Effects and Defects in Solids*, **159(4)**, 223-231.
- Singh K., I. Bala, V. Kumar (2009), Structural, optical and bioactive properties of calcium borosilicate glasses. *Ceramics International*, **35(8)**, 3401-3406
- Sebastian S., M.A. Khadar (2005), Microhardness indentation size effect studies in  $60\text{B}_2\text{O}_3\text{-(40-x)PbO-xMCl}_2$  and  $50\text{B}_2\text{O}_3\text{(50-x)PbO-xMCl}_2$  (M= Pb, Cd) glasses. *Journal of materials science*, **40(7)**, 1655-1659.
- Bhogi A., R.V. Kumar, P. Kistaiah (2015). Effect of alkaline earths on spectroscopic and structural properties of  $\text{Cu}^{2+}$  ions-doped lithium borate glasses. *Journal of non-crystalline solids*, **426**, 47-54.
- Zhao P., S. Kroeker, J.F. Stebbins (2000), Non-bridging oxygen sites in barium borosilicate glasses: results from  $^{11}\text{B}$  and  $^{17}\text{O}$  NMR. *Journal of Non-Crystalline Solids*, **276(1-3)**, 122-131.
- Springs G.A.C.M., G.P. Melis (1981), Refractive index and density of alkali lime borogermanosilicate glasses. *Journal of Materials Science*, **16(4)**, 1059-1062.
- ElBatal F.H., M.S. Selim, S.Y. Marzouk, M.A. Azooz (2007). UV-vis absorption of the transition metal-doped  $\text{SiO}_2\text{-B}_2\text{O}_3\text{-Na}_2\text{O}$  glasses. *Physica B: Condensed Matter*, **398(1)**, 126-134.
- Petrovskay T.S., (1997). Properties of lead borosilicate glasses: the effect of the structure. *Glass and ceramics*, **54(11-12)**, 347-350.
- Arora M., S. Baccaro, G. Sharma, D. Singh, K.S. Thind, D.P. Singh (2009). Radiation effects on  $\text{PbO-Al}_2\text{O}_3\text{-B}_2\text{O}_3\text{-SiO}_2$  glasses by FTIR spectroscopy. *Nuclear Instruments and Methods in Physics Research Section B: Beam Interactions with Materials and Atoms*, **267(5)**, 817-820.
- Ramkumar J., V. Sudarsan, S. Chandramouleeswaran, V.K. Shrikhande, G.P. Kothiyal, P.V. Ravindran, T. Mukherjee (2008), Structural studies on borosilicate glasses. *Journal of non-crystalline solids*, **354(15-16)**, 1591-1597.
- Sawvel A.M., S.C. Chinn, W.L. Bourcier, R.S. Maxwell (2005), Local structure of amorphous  $(\text{PbO})_x [(\text{B}_2\text{O}_3)_{1-z} (\text{Al}_2\text{O}_3)_z]_y (\text{SiO}_2)_y$  dielectric materials by multinuclear solid state NMR. *Chemistry of materials*, **17(6)**, 1493-1500.
- Van Uitert L.G., , D.A. Pinnow, J.C. Williams, T.C. Rich, R.E. Jaeger, W.H. Grodkiewicz (1973), Borosilicate glasses for fiber optical waveguides. *Materials Research Bulletin*, **8(4)**, 469-476.
- Ascencio J.A., A.C. Rincon, G. Canizal (2005), Synthesis and theoretical analysis of samarium nanoparticles: perspectives in nuclear medicine. *The Journal of Physical Chemistry B*, **109(18)**, 8806-8812.
- Ciobanu C.S., S.L. Iconaru, C.L. Popa, M. Motelica-Heino, D. Predoi, (2015). Evaluation of samarium doped hydroxyapatite, ceramics for medical application: Antimicrobial activity. *Journal of Nanomaterials*, **2015** | Article ID 849216 | [https:// doi.org/ 10.1155/ 2015/ 849216](https://doi.org/10.1155/2015/849216) .
- Kaur P., S. Kaur, G.P. Singh, D.P. Singh

- (2013), Sm<sup>3+</sup> doped lithium aluminoborate glasses for orange coloured visible laser host material. *Solid state communications*, **171**, 22-25.
20. Rouxel T., (2006), Elastic properties of glasses: a multiscale approach. *Comptes Rendus Mécanique*, **334(12)**, 743-753.
  21. Singh G.P., S. Kaur, P. Kaur, D.P. Singh (2012), Modification in structural and optical properties of ZnO, CeO<sub>2</sub> doped Al<sub>2</sub>O<sub>3</sub>-PbO-B<sub>2</sub>O<sub>3</sub> glasses. *Physica B: Condensed Matter*, **407(8)**, 1250-1255.
  22. Mhareb M.H.A., S. Hashim, S.K. Ghoshal, Y.S.M. Alajerami, M.A. Saleh, R.S. Dawaud, S.A.B Azizan (2014), Impact of Nd<sup>3+</sup> ions on physical and optical properties of Lithium Magnesium Borate glass. *Optical Materials*, **37**, 391-397.
  23. E.M. El-Khodary, A. Yassin (2010), Structural, optical, thermal and electrical studies on PVA/PVP blends filled with lithium bromide. *Curr Appl Phys*; **10(2)**, 607-13.
  24. Abdelghany A.M., M.A. Morsi, A. Abdelrazek, M.T. Ahmed (2018), Role of silica nanoparticles on structural, optical and morphological properties of poly (vinyl chloride-co-vinyl acetate-co-2-hydroxypropyl acrylate) copolymer. *Silicon*, **10(2)**, 519-524.
  25. Dimitrov V., S. Sakka (1996), Linear and nonlinear optical properties of simple oxides. II. *Journal of applied physics*, **79(3)**, 1741-1745.